chemosensors

Supplementary Material

Tetracycline antibiotics: elucidating the electrochemical fingerprint and oxidation pathway.

Rocío Cánovas,[1,2] Nick Sleegers,[1,2] Alexander L.N. van Nuijs,[3] Karolien De Wael*[,1,2]

[1] AXES Research Group, Bioscience Engineering Department, University of Antwerp, Groenenborgerlaan 171, 2020 Antwerp, Belgium.

[2] NANOlab Center of Excellence, University of Antwerp, Groenenborgerlaan 171, 2020 Antwerp, Belgium.

[3] Toxicological Center, University of Antwerp, Universiteitsplein 1, 2610 Antwerp, Belgium

***Corresponding author**: Karolien De Wael (karolien.dewael@uantwerpen.be)

chemosensors

Table of contents

Materials and Methods

LC-QTOF-MS conditions Reagents

Chromatographic separation was performed on a Luna C18 column (100 × 2.1 mm, 2.6 μm), maintained at room temperature, and using a mobile phase composed of 0.04% of formic acid in ultrapure water (A) and acetonitrile/ultrapure water (80/20, v/v) with 0.04% formic acid (B), in gradient. The gradient elution between the two solvents starts with 2% of solvent B and over the first following 13 min solvent B is linearly increasing up to 100%. From the 13.1 min to 15 min the eluent solely consist of solvent B, after that, at 15.1 min, the eluents re-equilibrate and come back to the initial 2% solvent B at the 19 min to re-calibrate the column. The flow rate and the injection volume were set at 0.3 mL/min and 1 μL, respectively. The instrument was operated in the 2 GHz (extended dynamic range) mode, which provides a full width at half-maximum (FWHM) resolution of approximately 4700 at *m*/*z* 118 and 10 000 at *m*/*z* 922. Positive polarity electrospray ionization (ESI) mode was used under the following specific conditions: gas temperature 300 °C; gas flow 8 L/min; nebulizer pressure 40 psi; sheath gas temperature 350 °C; sheath gas flow 11 L/min. Capillary and fragmentary voltages were set to 4000 and 135 V, respectively. A reference calibration solution (provided by Agilent Technologies) was continuously sprayed into the ESI source of the QTOF-MS system. The ions selected for recalibrating the mass axis, ensuring the mass accuracy throughout the run were *m*/*z* 121.0508 and 922.0097. The QTOF-MS device was acquiring from *m*/*z* 50 to 1000 in MS mode. Data-dependent acquisition mode (auto-MS/MS) was applied using two different collision energies (10 and 20 eV) for the fragmentation of the selected parent ions. The maximum number of precursors per MS cycle was set to 4 with minimal abundance of 2500 counts. In addition, precursor ions were excluded after every spectrum and released after 0.2 min.

chemosensors

Tables

Table S1. Maximum residue limit (MRL) for tetracyclines in animal tissues (COMMISSION REGULATION (EU) No 37/2010)

Antibiotics	Marker residue	Animal Species	MRL	Target Tissues	Other Provisions
Tetracycline	Sum of parent drug and its 4-epimer	All food-producing species	100 µg/kg 300 µg/kg 600 µg/kg 100 µg/kg 200 µg/kg	Muscle Liver Kidney Milk Eggs	For fin fish the muscle MRL relates to 'muscle and skin in natural proportions'. MRLs for liver and kidney do not apply to fin fish.
Doxycycline	Doxycycline	Bovine	100 µg/kg 300 µg/kg 600 µg/kg	Muscle Liver Kidney	Not for use in animals from which milk is produced for human consumption.
		Porcine, poultry	100 µg/kg 300 µg/kg 300 µg/kg 600 µg/kg	Muscle Skin & fat Liver Kidney	Not for use in animals from which eggs are produced for human consumption.
Oxytetracycline	Sum of parent drug and its 4-epimer	All food-producing species	100 µg/kg 300 µg/kg 600 µg/kg 100 µg/kg 200 µg/kg	Muscle Liver Kidney Milk Eggs	For fin fish the muscle MRL relates to 'muscle and skin in natural proportions'. MRLs for fat, liver and kidney do not apply to fin fish.
Chlortetracycline	Sum of parent drug and its 4-epimer	All food-producing species	100 µg/kg 300 µg/kg 600 µg/kg 100 µg/kg 200 µg/kg	Muscle Liver Kidney Milk Eggs	For fin fish the muscle MRL relates to 'muscle and skin in natural proportions'. MRLs for liver and kidney do not apply to fin fish.

** According to Article 14(7) of Regulation (EC) No 470/2009*

NOTE: the UE data differs from the U.S. Food and Drug Administration (FDA) that had set the MRLs for milk (0.4 mg kg^{-1}), fat (12 mg kg^{-1}), liver (6 mg kg^{-1}), and muscle (2 mg kg^{-1}) samples to control the levels of TCs satisfying the security value.[1–3]

chemosensors

Table S2. Summary of electrochemical biosensors based on aptamers, antibodies, molecular imprinted polymers and enzyme-linked immunoassays for tetracyclines (TCs) detection.

REF	TCs	Detection method	Electrode	Modification	LR	LOD	Recovery (%)
[4]	TET	PEC CV, EIS	Indium-Tin Oxides (ITO)	Aptamer TPP doped PFBT polymer quantum dots	0.1 – 1000 nM	0.26 nM	96 – 104
[5]	TET	PEC	FTO glass	Aptamer with zirconia (ZrO2) modified graphitic carbon nitride (g-C3N4) nanosheets	50 – 150 nM	8.7 nM	--
[6]	OXY	DPV	GCE	Aptamer covalently-bound via diazonium coupling reaction	2.17 nM – 0.2 mM	0.5 nM	87 – 99.3
[7]	TET	CV EIS DPV	Gold electrode	Aptamer linked to CNQDs and AgNPs nanocomposite	1 nM – 0.1mM	0.26 nM	96 – 103
[8]	TET	DPV EIS	Gold electrode	TET aptamer modified with Ferrocene based on β-cyclodextrin subject-object competition model	0.01 – 100 nM	0.008 nM	96 – 104.4
[9]	TET	DPV	modified carbon paste electrode	magnetic nanoparticles coated with MIP	0.08 – 80 μM	0.02 μM	78.5 – 101.6
[10]	OXY CHL DOXY	CV DPV	GCE	BMMIPs using Zein as crosslinker and Fe_3O_4 particles	0.025–500 μg/mL	0.025 μg/mL	83.73 – 95.97
[11]	OXY	CV DPV	paper-based printed elect.	capture anti-OXY antibody and OXY-conjugated BSA	2.17 – 434 nM	0.7 nM	--
[12]	TET	EIS	Gold electrode	antibody- terminated thiol layer self-assembled	6.27 – 0.56 nF μM	28 nM	98.5 – 106.9
[13]	TET DOXY	CV EIS	gold-coated silicon electrode	ultrathin PTA film modified with polyclonal antibodies	1 to 200 μg/L	0.01 μg/L	96 – 102
[14]	TET	LC-based aptasensor	-- (glass substrate)	label-free LC aptasensor	0.5–500 pM	0.5 pM	95.6 – 108.7
[15]	TET	EIS CV	SPCE	Anti-TET aptamer + prior pretreatment (LSV: 1 – 1.5V, H_2SO_4 0.5M)	0.11 – 45 nM	78.8 pM	87.8 – 97
[16]	TET	EIS and PEC	ITO	MCH/aptamer/AuInCN	0.01–500 nM	3.3 pM	99.6 – 110.6
[17]	TET	DPV	SPCE	MIOPPy and AuNPs	1 – 20 μM	0.65 μM	92.2 – 105
[18]	TET	CV, EIS, DPV	GCE	poly (L-glutamic acid)/MWCNTs for immobilization of anti-TET aptamer	0.1 fM – 1 μM	0.037 fM	94 – 95
[19]	TET	Fluorescence spectrophotometer	--	Aptamer + luminescence of SYBR Green I	11.3 – 56.3 μM	0.23 μM	98.98 – 104.67
[20]	TET	EIS and DPV	GCE	MoS2-TiO2@Au composite + thiolated DNA aptamer + biotin cDNA + avidin HRP	0.15 nM – 6 μM	0.05 nM	90 – 97
[21]	TET	PEC	ITO	aptasensor based on cerium doped CdS modified graphene (G)/$BiYWO_6$	0.45 nM- 2.25 μM	0.022 nM	103.8 – 105.3
[22]	TET	SPR	CM5 chip	Anti-TET aptamer on top of a DNA tetrahedron nanostructure	0.01–1000 μg/kg	0.0069 μg/kg	80.2 – 114.3
[23]	TET	DPV	SPCEs	APT 1: Fc and AuNPs nanocomposite APT 2: CNFs and AuNPs nanocomposite	22.5pM –2.25μM	0.74 nM	96 – 104
[24]	TET	CV	SPE	Aptasensor with ionic Liquid and Fe_3O_4 MNPs	1 nM – 10 mM	1 nM	84 – 92
[25]	TET	SWCSV	GCE	SbFE	0.40 – 3.00 μM	0.15 μM	91.5 – 109.7

[26]	TET	EIS	Gold electrode	label-free aptasensor	22.5nM – 6.75µM	22.5 nM	88.1 – 94.0
[27]	TET	CV, EIS, DPV	GCE	graphene oxide nanosheets + chemical immobilized aptamer	0.1 pM to 10 µM	29 fM	95 – 97
[28]	TET	DPV	Gold electrode	MNPs + CHI linker + Ab monoclonal	0.18 – 2.25 nM	72.2 pM	95.9 – 108
[29]	TET	DPV and CV	SPCE	Alginate film containing reduced graphene oxide and magnetite nanoparticles + aptamer	1 nM – 5 µM	0.6 nM	--
[30]	TET	[A]EIS [B]DPV	CPEs	[a]CPE/OA/anti-TET *versus* [b]MBCPE/Fe_3O_4NPs/OA/anti-TET	[Aa] 1pM – 0.1 µM [Ba]0.1nM–0.1 µM [Ab] 100pM – 1µM [Bb] 1 pM – 1 µM	[Aa] 0.3 pM [Ba] 29 pM [Ab] 3.8 fM [Bb] 0.31 pM	97–104 Serum 95 – 96 Honey 97 – 103 Milk
[31]	TET (DOXY)	CV characterization DPV measurement	SPGE	M-shape structure of aptamer (Apt)-CSs complex	1.5 nM – 3.5 µM	0.45 nM 0.74 nM milk 0.71 nM Ser	93.1–103.8 ser
[32]	TET	AdSDPV	Modified carbon paste electrode	carbon paste modified with 2.6% (w/w) of MWCNT-COOH and 3.1% (w/w) of GO	20 – 310 µM	0.36 µM	92 – 103
[33]	TET	CV and EIS	GCE	AuNPs + anti-TET aptamer + MB	0.1nM – 1mM	4.2 pM	96 – 108
[34]	TET	PEC EIS	F-doped SnO2 conducting glass	Graphitic Carbon Nitride Sensitized with CdS Quantum Dots + aptamer	10–250 nM	5.3 nM	99.1 – 101.1
[35]	TET	Colorimetric assay	-- (Cuvette)	Aptasensor with cysteamine-stabilized AuNPs	0.45nM – 4.5 µM	87.7 nM	91.28 –100.87
[36]	TET (DOXY)	Absorbance, colorimetric assay	-- (Microplate reader)	Aptasensor THMS and AuNPs	0.3 – 10 nM	266 pM	--
[37]	TET	Absorbance, direct competitive enzyme-linked aptamer assay (dc-ELAA)	-- (Plate)	ssDNA aptamer	0.225nM–2.25µM	0.22 nM	92.09 – 109.7
[38]	TET	Immunoassay	GCE	AuNPs + monoclonal Ab onto CdS nanoclusters	22.5pM–112.5µM	0.016 pM	88 – 107
[39]	TET	Absorbance, Indirect competitive enzyme-linked aptamer assay (ic-ELAA)	-- (Microplate reader)	ssDNA aptamer	22.5 – 225nM	21.6 nM	95.38 –108.07
[40]	TET	EIS DPV	Gold electrode	Covalent attachment of amino-modified APT	11.3nM – 11.3µM	2.25 nM	90 – 95.7
[41]	TET	DPV	GCE	PB-CHI-glutaraldehyde system + AuNPs + anti-TET aptamer	1 nM – 10 mM	0.32 nM	92 – 106
[42]	TET	LSV	Gold electrode	platinum-catalyzed HER with anti-TC antibody	0.112– 225 nM	0.013 nM	86 – 110 H 95.6 – 118 M 98 – 106.7 P
[43]	TET TET OXY CHL DOXY	Amperometry Competitive immunoassay using TC-HRP on antiTC-modified MBs	SPCE	ProtG-MBs + anti-TET Ab + HQ mediator and H_2O_2 detection	12.5–676.2 ppb 17.8–189.6ng/mL 4–242.3 ng/mL 144.2–2001.9 2.6–234.9	3.9ppb(ng/mL) 1.9″/8.9ng/mL 1.2 ng/mL 66.8 ng/mL 0.7 ng/mL	99
[44]	TET, OXY, DOXY, CHL, DEME	ELISA	SPCE	AuNPs conjugated with polyclonal anti-TET Ab (TMB/H_2O_2 + TET-HRP)	0 – 250 ppb	10 ppb	70 – 95
[45]	TET	EIS	PS chip	Aptamer PS biosensor	2.1 – 62.4 nM	2 nM	--
[46]	TET	CV DPV	GCE	Ethanolamine + TET aptamer + MWCNTs-COOH	10 nM – 50 µM	5 nM	88 – 96
[47]	TET	CV (EIS)	GCE	MIP CNT-AuNPs	0.1– 40 mg/L	0.04 mg/L	--
[48]	TET OXY	CV SWV	SPGE	Biotinylated ssDNA aptamer interaction with streptavidin	10 nM – 10 µM --	10 nM	--

	DOXY				--		
[49]	TET	ELISA	-- (Immuno plate)	(biotin-avidin)	0.316 – 316 nM	10 nM	~ 90
[50]	TET OXY CHL	ELISA	--	anti-TC antibodies	0.1– 100 µg/mL	0.01 µg/mL	74 – 116
[3]	TET	ELISA	--	Haptens	1.15 – 38.9 ng/mL	0.4 ng/mL	79 – 108

TET: tetracycline, DOXY: doxycycline, OXY: oxytetracycline, CHL: chlortetracycline, MNC: minocycline, DEME: demeclocycline, PEC: photoelectrochemical; TPP: tetraphenyl porphyrin; FTO: fluorine doped tin oxide; EIS: electrochemical impedance spectroscopy, CV: cyclic voltammetry, DPV: differential pulse voltammetry, BSA: bovine serum albumin, PTA: polytyramine, LSV: linear sweep voltammetry, SPR: surface plasmon resonance, SPCE: screen-printed carbon electrode, GCE: glassy carbon electrode, SPGE: screen-printed gold electrode, CPEs: carbon paste electrodes, SWCSV: square-wave cathodic stripping voltammetry, Ab: antibody; BMMIPs: biocompatible magnetic molecularly imprinted polymers; AgNPs: silver nanoparticles; CNQDs: carbon nitride quantum dots; LC: liquid crystal; MCH: mercaptohexanol; AuInCN; plasmon Au coupling with MOF-derived In_2O_3@g-C_3N_4 nanoarchitectures; MIOPPy: molecularly imprinted overoxidized polypyrrole, Fc: ferrocene AuNPs: gold nanoparticles, CNFs: carbon nanofibers, SbFE: antimony film electrode, MNPs: carboxyl-Fe3O4 nanoparticle, CHI: chitosan, MB: methylene blue, THMS: triple-helix molecular switch, HER: hydrogen evolution reaction, HQ: hydroquinone, H_2O_2: hydrogen peroxide, PS: nanoporous silicon, ELISA: enzyme-linked immunosorbent assay.

Table S3. Summary of electrochemical approaches based on modified electrodes for tetracycline determination.

REF	TCs	Detection Method	Electrode	Modification	LR	LOD	Recovery (%)
[51]	TET	EIS	pencil graphite electrode	reduced graphene oxide and AuNPs	0.1 fM – 1 µM	30 aM	92 – 102
[52]	TET DOXY OXY CHL	AdTDPV	Graphene-based SPE	Electrochemically reduced graphene oxide	20 – 80 µM	12 µM	94 – 110
[53]	TET	CV DPV EIS	GCE	zirconium ferrate doped silver phosphate sensor	10 – 90 nM	6.38 nM	--
[54]	DEME	SW-AdSV	BDDE	unmodified	10 – 90 and 1 – 50 µg/mL	0.24 – 1.17 µg/mL	103 – 109
[55]	TET	CV and EIS SW-AdSV	GCE	poly(malachite green)	5 – 100 µM	1.6 µM	98.49 – 99.78
[56]	TET	CV and EIS polyclonal Ab-TC	Gold microelectrodes	TC immobilized in the µWE by 3 ≠ methods, Py/Py-COOH/MNPs	0.22 pM – 2.25 nM	2.7 pM	--
[57]	TET	DPV	60% graphite-PU composite electrode	Deproteinization and extraction of the antibiotic by SPE	3.8 – 38 µM peak1 3.8 – 19 µM peak2	2.6 µM	83 – 99 (bov) 83 – 97 (bre)
[58]	TET (UA)	CV DPV	GCE	p-Mel film on ERGO	5 – 225 µM	2.2 µM	99 – 99.6 99.7 – 99.9
[59]	TET	CV DPV	GCE	PtNPs	9.99 – 44.01 µM	4.28 µM	--
[60]	TET OXY	DPV	Graphite composite electrode	60% graphite-PU composite	3.8–38 µM 3.8–28.5 µM	2.3 µM 1.6 µM	98 96 – 97
[61]	TET	DPV, CV and EIS	GCE	Fe/Zn–MMT catalyst	0.3 – 52 µM	10.7 nM	97.2 – 103
[62]	TET	SWV Urine, serum, milk	SPGE	SAM of Cys on AuNP	4 – 800 µM U 4 – 700 µM S 4 – 700 µM M	0.4 µM U 0.5 µM S 0.5 µM M	93 U 107 S 113 M
[63]	TET (SA)	SWV	SPdCEs (*dual*)	ProtG-4-ABA film grafted + HRP and HQ	6.4 – 385 nM	1.93 nM	98 ± 6
[64]	TET	DPV	GPU electrode	GPU composite	4 – 40 µM	2.8 µM	92.6 – 100

[65]	TET	CV	Gold microelectrode (GME)	Electrodeposition of gold colloids on the tungsten tip	2.08 – 20.8 µM	187 nM	--
[66]	MNC OXY TET DEME CHL DOXY	LC + SPE Amperometric detector operating under: DC (direct amperometric detection) and IPAD (complex multiple potential waveform)	Polycrystalline gold electrode	--	Under IPAD: 0.25 – 263 mg/L Under DC: 0.04 – 7.1 mg/L	50 – 150 nM 0.5 – 0.9 µM	70 – 118
[67]	TET	LSV	GCE	Ionic liquid-MWCNT paste film coating	0.11 – 22 µM	30 nM	91 – 105
[68]	TET OXY CHL	FIA + CV Dc amperometry	SPGE	--	1 – 500 µM 5 – 50 µM 1 – 500 µM	0.96 µM 0.35 µM 0.58 µM	83.4 – 99.3 85.9 – 99.2 88.7 – 100.3
[69]	TET OXY DOXY CHL	CV HPLC-ED	GCE	MWCNTs	2.5 – 100 µM 2.5 – 100 µM 1 – 100 µM 1 – 100 µM	0.12 µM 0.09 µM 0.44 µM 0.31 µM	99 95 93 87
[70]	DEME OXY TET	Multi IPAD + HPLC	Gold electrode (Detection cell)	--	0.1 – 15 mg/L 0.21–3.1 µM 0.1 – 15 mg/L 0.1 – 15 mg/L	0.07 mg/L 0.10–0.17 0.08 0.05	102.5 117 111
[71]	OXY TET CHL DOXY	CV HPLC	BDD and GCE	Ni-DIA	0.05–100 ng/ml 0.1–201 µM 0.05 –100 0.1 –100 0.1 –100	0.01 0.02–0.10 0.01 0.05 0.05	83.3 – 102.5 85.9 – 97 86 – 97.9 88.4 – 103.7
[72]	TET CHL DOXY OXY	CV, HPLC + PAD	BDDE	Anodized BDD thin film electrode	0.1 – 100 µg/mL	0.05µg/mL 0.1 µg/mL 0.1 µg/mL 0.05µg/mL	70.8 – 96
[73]	TET	Indirect potentiometric detection through microbial inhibition	CO_2 sensor	--	50 – 100 µg/L 348 to 6600 ppm	25 µg/L	--
[74]	OXY TET CHL MTC DOXY	HPLC + coulometric electrode array system	ESA electrochemical detector (4 electrodes)	(*) samples pretreated using liquid–liquid extraction based on hexane	0.10–2.08 µM	0.026–0.052 µM	92.2 – 96.2 89.6 – 93.9 88.4 – 92.9 92.5 – 94.4 91.1 – 94.2
[75]	TET OXY CHL DOXY	CV and LCEC	GCE	Ru oxide – Ru cyanide films	--	0.1 ppm 0.1 ppm 0.5 ppm 0.5 ppm	73 – 111
[76]	TET DOXY OXY CHL	FI-ED CV HV	BDDE (GCE)	As-deposited BDD Anodized BDD	0.1 – 50 mM (TET) 0.5 – 50 mM (DOXY, OXY and CHL)	10 nM	99.8 % 98.4 % 101.85 % 99.87 %
[77]	TET	CV	Acetylene black electrode	Ac black electrode SDS on the surface	0.12 – 60 µM	12 nM	98.2 – 105
[78]	DOXY CHL	PAD CV	Au rotating disk electrode	--	1 – 100 µM	1 µM	87–103 93–109
[79]	OXY	FI-ED CV and SWV	CFME	--	1 – 100 µM	0.29 µM (SWV)	96 (milk) 91 (eggs)
[80]	TET	FI + PAD CV (Au RDE)	Gold rotating disk electrode	--	5 µM – 0.6 mM	1 µM	--
[81]	TET OXY CHL	CE+CV	Hg-film µm electrode	--	1 – 500 µM (TET, CHL) 2.5 – 800 µM (OXY)	0.7 µM (TET, CHL) 1.5 µM (OXY)	--
[82]	CHL, DEME, DOXY, MTC, MNC, OXY	HPLC + amperometric detection (ECD) at 1.2 V	GCE	--	0.1 – 50 ng/µL DC, MNC, OTC (0.21–104 µM) and TC 0.5 – 50 ng/µL for CTC, DMC and MTC	0.20–2.0 µM	99.1 – 100.4

	TET						
[83]	TET DOXY OXY CHL	FI-ED Voltammetric characterization and Flow Injection Detection	Ni-GCE	Nickel modified	5.6 – 180 µM 5.6 – 225 µM 5.4 – 217 µM 5.2 – 208 µM	67.5 nM 2.07 µM 73 µM 3.78 µM	99.6 101.78 101.2 98.6
[84]	OXY TET DOXY CHL	CV DPV LCEC	GCE Pretreated (PGCE)	Pretreatment in PB +1.8 V 5min and -1.2 V 10 seconds	0.2 – 400 ng 0.2 – 400 ng 4 ng – 2 µg 1.2 ng – 1.6 µg	0.2 ng 0.2 ng 4 ng 1.2 ng	-- -- -- --
[85]	OXY	DPP Urine and human serum	DME	--	6.5 – 98 µM U 9.5 – 1200µM S	5.5 µM for both fluids	80 % (U) 85 % (S)
[86]	TET OXY	FI Amperometric Det.	three-electrode thin-layer flow-through cell	detector based on ion transfer across a water - solidified nitrobenzene	2 – 200 µM 5 – 300 µM	20 ng 50 ng	--
[87]	TET HCl with Anhydrous TET	DPP	Old capillary mercury drops (Taccussel PRG five-pulse polarograph)	--	--	--	99 – 102.3
[88]	OXY	DPASV	HMDE (hanging mercury drop electrode)	--	5 nM – 100 µM	2 nM	--
[89]	OXY	CV LCS-CP	--	--	10 – 100 µg/mL	5 µg/mL	--
[90]	TET, RTC, DEME, MNC, MTC, DOXY, LMC	CV Acetate buffer, pH 4 and pH 5.6	Pt/Au rotating disk electrodes	--	--	5 mM	--

TET: tetracycline, DOXY: doxycycline, OXY: oxytetracycline, CHL: chlortetracycline, DEME: demeclocycline, MNC: minocycline, MTC: methacycline, LMC: lymecycline, RTC: roletetracycline, AdTDPV: adsorptive transfer stripping differential pulse voltammetry; EIS: electrochemical impedance spectroscopy, CV: cyclic voltammetry, DPV: differential pulse voltammetry, LSV: linear sweep voltammetry, SPR: surface plasmon resonance, SPE: screen printed electrode; SPCE: screen-printed carbon electrode, GCE: glassy carbon electrode, SPGE: screen-printed gold electrode, SWCSV: square-wave cathodic stripping voltammetry, Ab: antibody; SW-AdSV: square wave adsorptive striping voltammetry, BDDE: boron-doped diamond electrode, SPE: solid-phase extraction, pMel: polymelamine, ERGO: electrochemically reduced graphene oxide, Fe/Zn–MMT: iron/zinc cation–exchanged montmorillonite, SAM: Self-assembly monolayer, GPU: graphite polyurethane, Ni-DIA: nickel-implanted boron-doped diamond thin film electrode, SDS: sodium dodecyl sulfate, DPP: differential pulse polarography/voltammetry.

Table S4. LC-QTOF data for all four TCs and the three main oxidation products.

Compounds	Retention time (min)	Measured *m/z*	Theoretical *m/z*	Error	Chemical formula	Potential applied (pH 9)		Potential applied (pH 4)	
						0.66 V	0.85 V	0.80 V	1.00 V
DOXY	5.60	445.1603	445.1605	-0.55	$C_{22}H_{24}N_2O_8$				
OXY	4.58	561.1557	461.1555	0.53	$C_{22}H_{24}N_2O_9$				
TET	4.72 / (4.25)	445.1608	445.1605	0.58	$C_{22}H_{24}N_2O_8$				
CHL	5.44/ 4.89	479.1233	479.1216	3.62	$C_{22}H_{23}ClN_2O_8$				
Oxidation Product 1 (-14 Da)									
D1	5.50	431.1454	431.1449	1.18	$C_{21}H_{22}N_2O_8$	x		x	
O1	4.48	447.1403	447.1398	1.11	$C_{21}H_{22}N_2O_9$	x		x	
T1	4.45/ (4.19)	431.1454	431.1449	1.18	$C_{21}H_{22}N_2O_8$	x		x	
C1	5.23	465.1059	465.1059	-0.04	$C_{21}H_{21}ClN_2O_8$	x		x	
Oxidation Product 2 (+ 16 Da)									
D2	4.79	461.1582	461.1555	5.96	$C_{22}H_{24}N_2O_9$		x		x
O2	3.92	477.1504	477.1504	0.06	$C_{22}H_{24}N_2O_{10}$		x		x
T2	4.54/ (4.06)/(3.80)	461.1554	461.1555	-0.12	$C_{22}H_{24}N_2O_9$		x		x
C2	5.68	495.1164	495.1165	-0.17	$C_{22}H_{23}ClN_2O_9$		x		x
Oxidation Product 3 (+ 14 Da)									
D3	5.01 / 5.91	459.1399	459.1398	0.2	$C_{22}H_{22}N_2O_9$		x		x
O3	4.65	475.1348	475.1347	0.17	$C_{22}H_{22}N_2O_{10}$		x		x
T3	4.98	459.1404	459.1398	1.29	$C_{22}H_{22}N_2O_9$		x		x
C3	5.68	493.1011	493.1008	0.54	$C_{22}H_{21}ClN_2O_9$		x		x

Figures

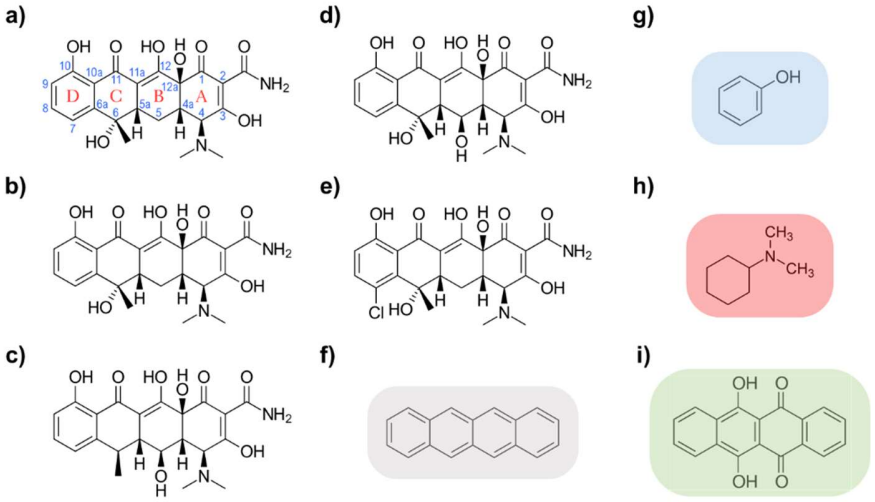

Figure S1. a) Skeletal formula of tetracycline with atoms and four rings numbered and labeled. Chemical structure of the tetracycline antibiotics studied in this work: **b)** TET, **c)** DOXY, **d)** OXY and **e)** CHL; and the chemical compounds used to verify the oxidation peaks along the electrochemical fingerprints in the pH screening: **f)** naphthacene core, **g)** phenol, **h)** N,N-dimethylcyclohexylamine and **i)** 6,11-dihydroxy-5,12-naphthacenedione.

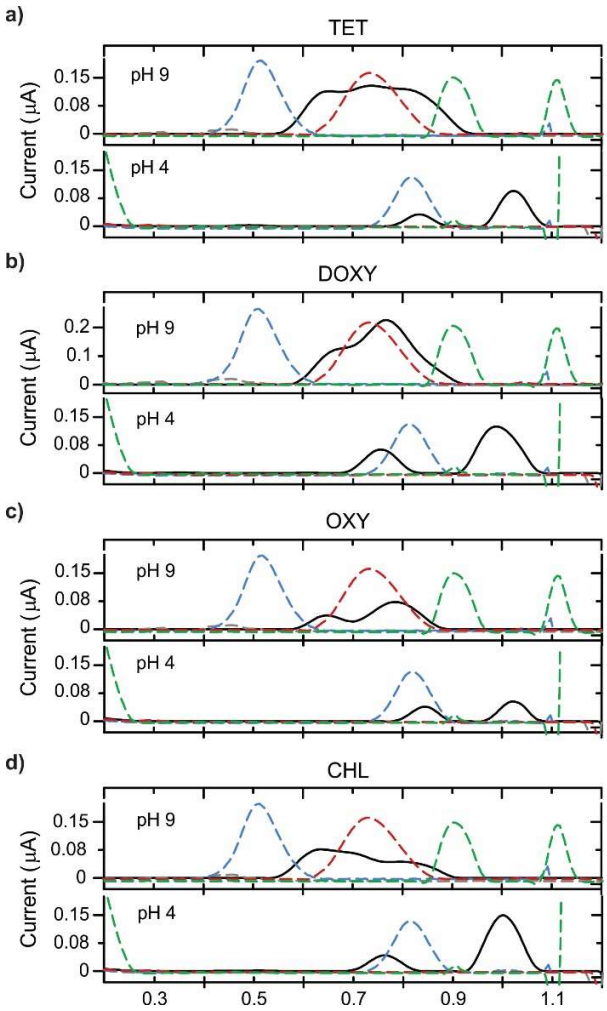

Figure S2. Square wave voltammograms (baseline-corrected) obtained at pH 4 and 9 of Britton Robinson buffer of all TCs (black line) **a)** TET, **b)** DOXY, **c)** OXY and **d)** CHL at 10 μM concentration each. Phenol (blue dashed line), benz[b]anthracene (grey dashed line) and N,N-dimethylcyclohexylamine (red dashed line) in a concentration of 10 μM and 6,11-dihydroxy-5,12-naphthacenedione (green dashed line) in a concentration of 1 mM.

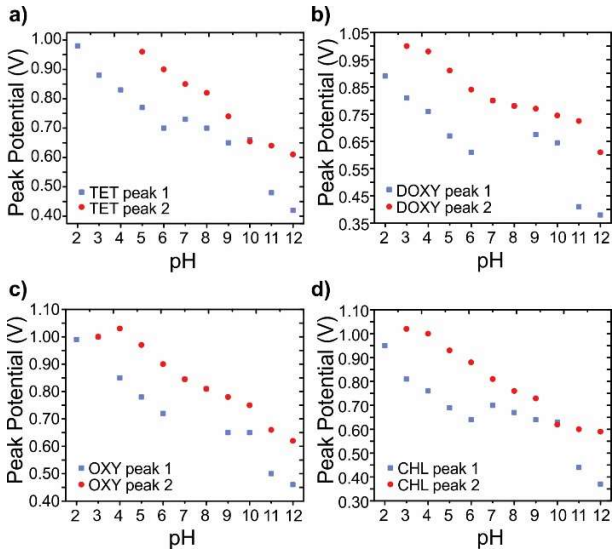

Figure S3. Peak potential of the first peak (in blue squares) and second peak (red circles) *versus* pH of **a)** TET, **b)** DOXY, **c)** OXY and **d)** CHL. The third peak is not included due to its less evident presence within the pH range.

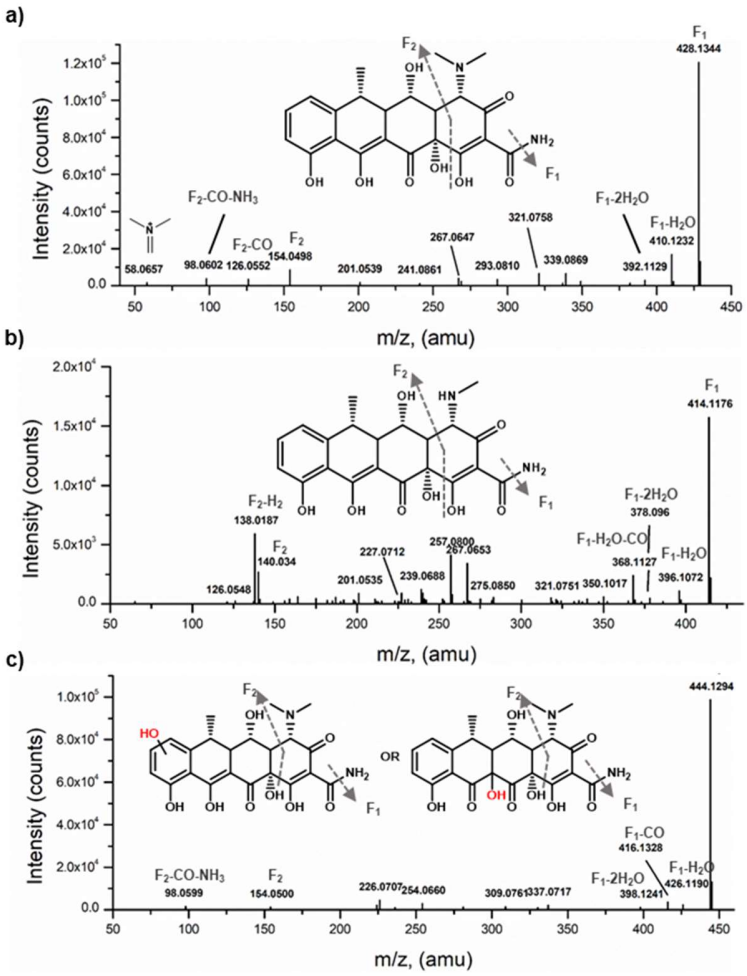

Figure S4. MS/MS spectra of **a)** DOXY (*m*/*z* 445.1650, $C_{22}H_{24}N_2O_8$), **b)** oxidation product D_1 (*m*/*z* 431.1454, $C_{21}H_{22}N_2O_8$), **c)** oxidation product D_2 (*m*/*z* 461.1558, $C_{22}H_{24}N_2O_9$).

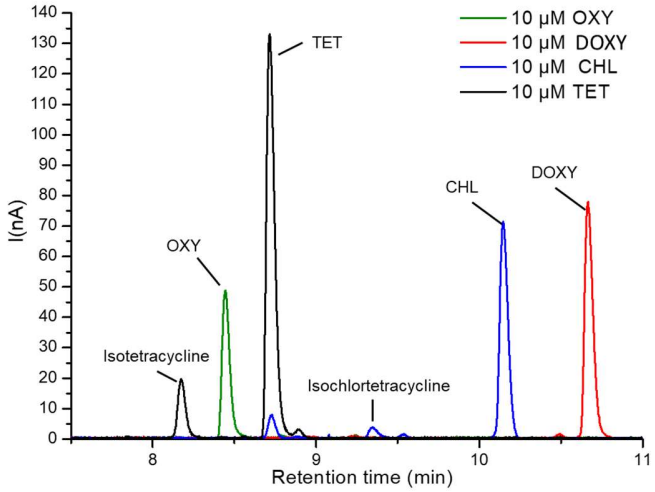

Figure S5. HPLC–ECD chromatograms of 10 µM TET (black), CHL (blue), OXY (green) and DXC (red) at 1.0 V.

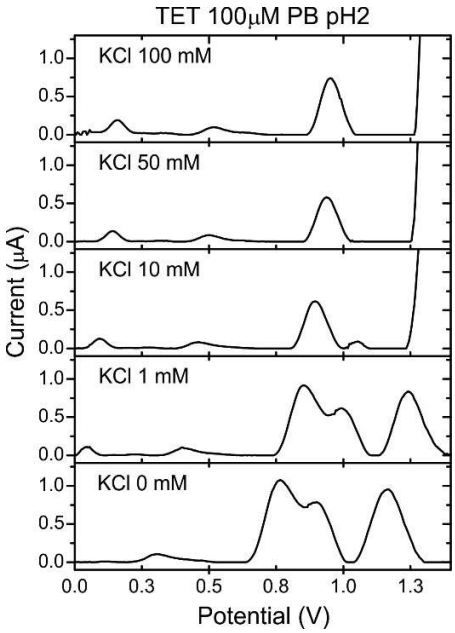

Figure S6. Electrochemical influence of the supporting electrolyte (concentration of 0, 1, 10, 50 and 100 mM) at pH 2 using a solution of tetracycline (TET) 100 μM in phosphate buffer (PB).

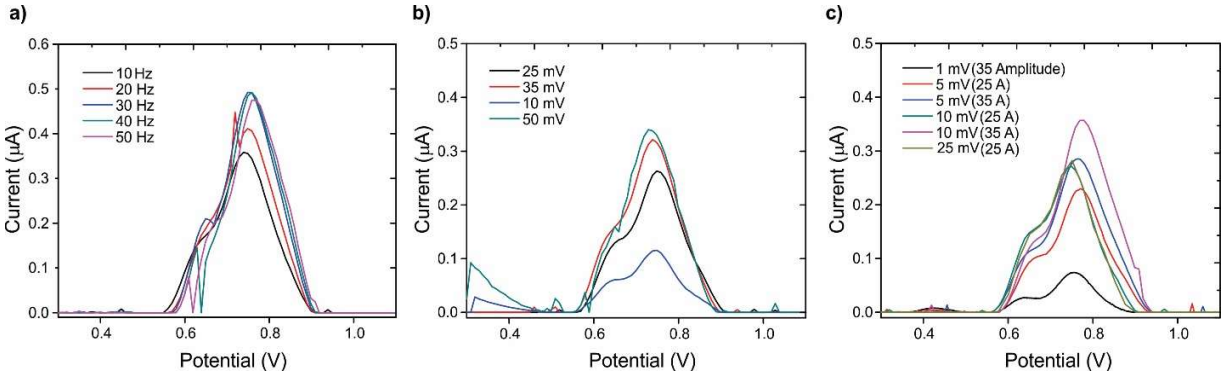

Figure S7. Optimization of the main parameters used in square wave voltammetry: **a)** Frequency (Hz), **b)** Amplitude (mV) and **c)** step potential (mV). The step potential was compared with regard to the best options of amplitude (25 and 35 mV) in order to select the optimal option.

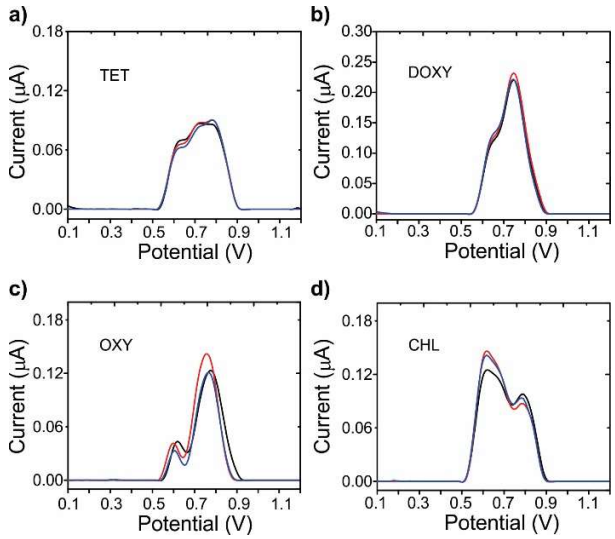

Figure S8. Reproducibility study (N=3) by square wave voltammetry (baseline-corrected) of each tetracycline 10 μM concentration at pH 9, **a)** TET, **b)** DOXY, **c)** OXY and **d)** CHL.

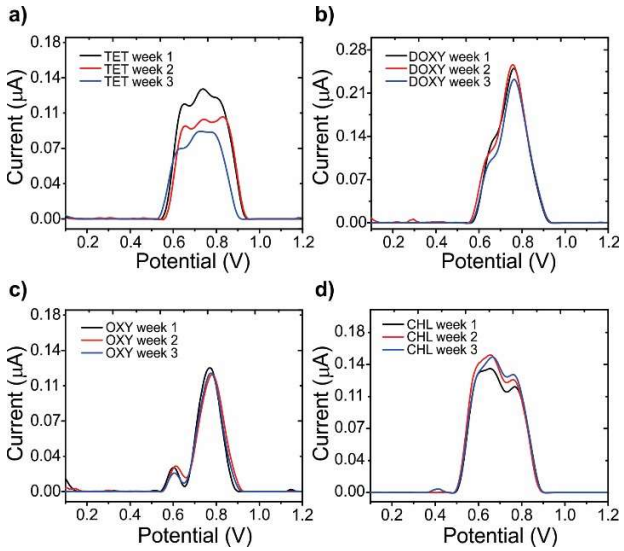

Figure S9. Stability of the different stocks solutions with time (after 1, 2 and 3 weeks) **a)** TET, **b)** DOXY, **c)** OXY and **d)** CHL.

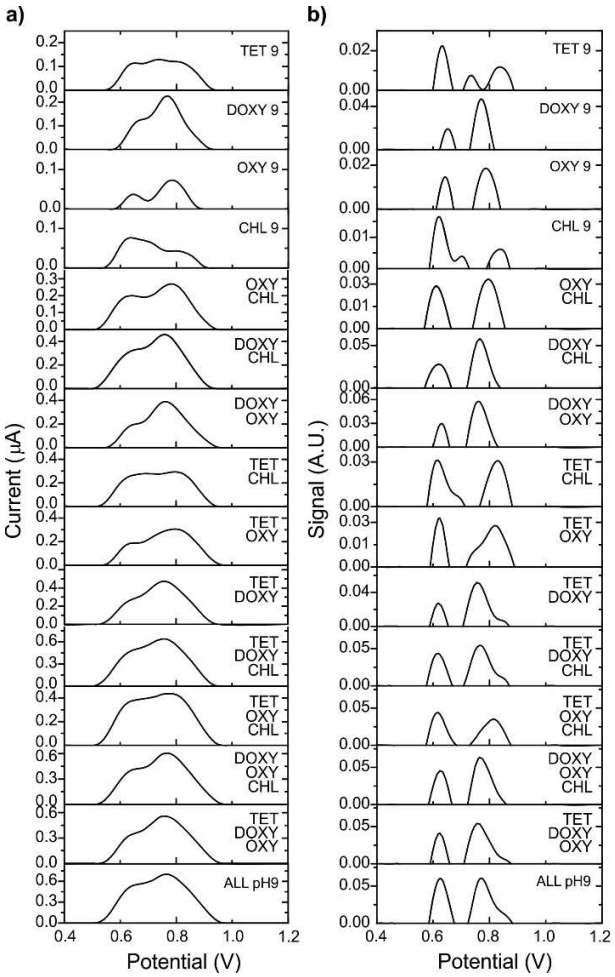

Figure S10. Data treatment with Matlab script to improve peak separation/identification at pH 9 for single TCs and all combination in mixtures of TCs **a)** square wave voltammetry from raw data (corrected by moving average) and **b)** output signal after the application of the script.

References

1. Liu, X.; Huang, D.; Lai, C.; Zeng, G.; Qin, L.; Zhang, C.; Yi, H.; Li, B.; Deng, R.; Liu, S.; et al. Recent advances in sensors for tetracycline antibiotics and their applications. *TrAC - Trends Anal. Chem.* **2018**, *109*, 260–274, doi:10.1016/j.trac.2018.10.011.
2. Oka, H.; Ito, Y.; Matsumoto, H. Chromatographic analysis of tetracycline antibiotics in foods. *J. Chromatogr. A* **2000**, *882*, 109–133, doi:10.1016/S0021-9673(99)01316-3.
3. Pastor-Navarro, N.; Morais, S.; Maquieira, Á.; Puchades, R. Synthesis of haptens and development of a sensitive immunoassay for tetracycline residues. Application to honey samples. *Anal. Chim. Acta* **2007**, *594*, 211–218, doi:10.1016/j.aca.2007.05.045.
4. Piaopiao, C.; Yichen, X.; Xiaoxiao, C.; Shan, Z.; Yang, L.; Chaobiao, H. A " Signal On " Photoelectrochemical Aptasensor For Tetracycline Detection Based On Semiconductor Polymer Quantum Dots. *J. Electrchemical Soc.* **2020**, *167*, 067516, doi:10.1149/1945-7111/ab818a.
5. Zarei, M. Sensitive visible light-driven photoelectrochemical aptasensor for detection of tetracycline using ZrO2/g-C3N4 nanocomposite. *Sensors Int.* **2020**, *1*, 100029, doi:10.1016/j.sintl.2020.100029.
6. Yang, Y.; Yan, W.; Guo, Y.; Wang, X.; Zhang, F.; Yu, L.; Guo, C.; Fang, G. Sensitive and selective electrochemical aptasensor via diazonium-coupling reaction for label-free determination of oxytetracycline in milk samples. *Sensors and Actuators Reports* **2020**, *2*, 100009, doi:10.1016/j.snr.2020.100009.
7. Hu, X.; Xu, Y.; Cui, X.; Li, W.; Huang, X.; Li, Z.; Shi, J.; Zou, X. Fluorometric and electrochemical dual-mode nanoprobe for tetracycline by using a nanocomposite prepared from carbon nitride quantum dots and silver nanoparticles. *Microchim. Acta* **2020**, *187*, 1–10.
8. Wu, Y.; Bi, H.; Ning, G.; Xu, Z.; Liu, G.; Wang, Y.; Zhao, Y. Cyclodextrin subject-object recognition-based aptamer sensor for sensitive and selective detection of tetracycline. *J. Solid State Electrochem.* **2020**, *24*, 2365–2372.
9. Pizan-Aquino, C.; Wong, A.; Aviles-Felix, L.; Sotomayor, M.D.P.T. Evaluation of the performance of selective M-MIP to tetracycline using electrochemical and HPLC-UV method. *Mater. Chem. Phys.* **2020**, *245*, 122777, doi:10.1016/j.matchemphys.2020.122777.
10. Wang, S.; Ma, R.; Mazzu, Y.Z.; Zhang, J.; Li, W.; Tan, L.; Zhou, L.-D.; Xia, Z.-N.; Zhang, Q.-H.; Yuan, C.-S. Specific adsorption of tetracycline from milk by using biocompatible magnetic molecular imprinting material and evaluation by ECD. *Food Chem.* **2020**, *326*, 126969, doi:10.1016/j.foodchem.2020.126969.
11. Jampasa, S.; Pummoree, J.; Siangproh, W.; Khongchareonporn, N.; Bgamrojanavanich, N.; Chailapakul, O.; Chaiyo, S. Chemical " Signal-On " electrochemical biosensor based on a competitive immunoassay format for the sensitive determination of oxytetracycline. *Sensors Actuators B. Chem.* **2020**, *320*, 128389, doi:10.1016/j.snb.2020.128389.
12. Starzec, K.; Cristea, C.; Tertis, M.; Feier, B.; Wieczorek, M.; Koscielniak, P.; Kochana, J. Employment of electrostriction phenomenon for label-free electrochemical immunosensing of tetracycline. *Bioelectrochemistry*

2020, *132*, 107405, doi:10.1016/j.bioelechem.2019.107405.

13. Prusty, A.K.; Bhand, S. A capacitive immunosensor for tetracycline estimation using antibody modified polytyramine-alkanethiol ultra-thin film on gold. *J. Electroanal. Chem.* **2020**, *863*, 114055, doi:10.1016/j.jelechem.2020.114055.
14. Rouhbakhsh, Z.; Verdian, A.; Rajabzadeh, G. Design of a liquid crystal-based aptasensing platform for ultrasensitive detection of tetracycline. *Talanta* **2020**, *206*, 120246, doi:10.1016/j.talanta.2019.120246.
15. Alawad, A.; Istamboulié, G.; Calas-Blanchard, C.; Noguer, T. A reagentless aptasensor based on intrinsic aptamer redox activity for the detection of tetracycline in water. *Sensors Actuators, B Chem.* **2019**, *288*, 141–146, doi:10.1016/j.snb.2019.02.103.
16. Feng, Y.; Yan, T.; Wu, T.; Zhang, N.; Yang, Q.; Sun, M.; Yan, L.; Du, B.; Wei, Q. A label-free photoelectrochemical aptasensing platform base on plasmon Au coupling with MOF-derived In2O3@g-C3N4 nanoarchitectures for tetracycline detection. *Sensors Actuators, B Chem.* **2019**, *298*, 126817, doi:10.1016/j.snb.2019.126817.
17. Devkota, L.; Nguyen, L.T.; Vu, T.T.; Piro, B. Electrochemical determination of tetracycline using AuNP-coated molecularly imprinted overoxidized polypyrrole sensing interface. *Electrochim. Acta* **2018**, *270*, 535–542, doi:10.1016/j.electacta.2018.03.104.
18. Benvidi, A.; Yazdanparast, S.; Rezaeinasab, M.; Tezerjani, M.D.; Abbasi, S. Designing and fabrication of a novel sensitive electrochemical aptasensor based on poly (L-glutamic acid)/MWCNTs modified glassy carbon electrode for determination of tetracycline. *J. Electroanal. Chem.* **2018**, *808*, 311–320, doi:10.1016/j.jelechem.2017.12.032.
19. Yang, C.; Bie, J.; Zhang, X.; Yan, C.; Li, H.; Zhang, M.; Su, R.; Zhang, X.; Sun, C. A label-free aptasensor for the detection of tetracycline based on the luminescence of SYBR Green I. *Spectrochim. Acta - Part A Mol. Biomol. Spectrosc.* **2018**, *202*, 382–388, doi:10.1016/j.saa.2018.05.075.
20. Tang, Y.; Liu, P.; Xu, J.; Li, L. Le; Yang, L.; Liu, X.; Liu, S.; Zhou, Y. Electrochemical aptasensor based on a novel flower-like TiO2 nanocomposite for the detection of tetracycline. *Sensors Actuators, B Chem.* **2018**, *258*, 906–912, doi:10.1016/j.snb.2017.11.071.
21. Han, Q.; Wang, R.; Xing, B.; Chi, H.; Wu, D.; Wei, Q. Label-free photoelectrochemical aptasensor for tetracycline detection based on cerium doped CdS sensitized BiYWO6. *Biosens. Bioelectron.* **2018**, *106*, 7–13, doi:10.1016/j.bios.2018.01.051.
22. Wang, S.; Dong, Y.; Liang, X. Development of a SPR aptasensor containing oriented aptamer for direct capture and detection of tetracycline in multiple honey samples. *Biosens. Bioelectron.* **2018**, *109*, 1–7, doi:10.1016/j.bios.2018.02.051.
23. Xu, Q.; Liu, Z.; Fu, J.; Zhao, W.; Guo, Y.; Sun, X.; Zhang, H. Ratiometric electrochemical aptasensor based on ferrocene and carbon nanofibers for highly specific detection of tetracycline residues. *Sci. Rep.* **2017**, *7*, 2–11, doi:10.1038/s41598-017-15333-5.

24. Shi, Z.; Hou, W.; Jiao, Y.; Guo, Y.; Sun, X.; Zhao, J.; Wang, X. Ultra-sensitive aptasensor based on IL and Fe3O4 nanoparticles for tetracycline detection. *Int. J. Electrochem. Sci.* **2017**, *12*, 7426–7434, doi:10.20964/2017.08.76.
25. Krepper, G.; Pierini, G.D.; Pistonesi, M.F.; Di Nezio, M.S. "In-situ" antimony film electrode for the determination of tetracyclines in Argentinean honey samples. *Sensors Actuators, B Chem.* **2017**, *241*, 560–566, doi:10.1016/j.snb.2016.10.125.
26. Le, T.H.; Pham, V.P.; La, T.H.; Phan, T.B.; Le, Q.H. Electrochemical aptasensor for detecting tetracycline in milk. *Adv. Nat. Sci. Nanosci. Nanotechnol.* **2016**, *7*, doi:10.1088/2043-6262/7/1/015008.
27. Benvidi, A.; Tezerjani, M.D.; Moshtaghiun, S.M.; Mazloum-Ardakani, M. An aptasensor for tetracycline using a glassy carbon modified with nanosheets of graphene oxide. *Microchim. Acta* **2016**, *183*, 1797–1804, doi:10.1007/s00604-016-1810-y.
28. Liu, X.; Zheng, S.; Hu, Y.; Li, Z.; Luo, F.; He, Z. Electrochemical Immunosensor Based on the Chitosan-Magnetic Nanoparticles for Detection of Tetracycline. *Food Anal. Methods* **2016**, *9*, 2972–2978, doi:10.1007/s12161-016-0480-z.
29. Zhan, X.; Hu, G.; Wagberg, T.; Zhan, S.; Xu, H.; Zhou, P. Electrochemical aptasensor for tetracycline using a screen-printed carbon electrode modified with an alginate film containing reduced graphene oxide and magnetite (Fe3O4) nanoparticles. *Microchim. Acta* **2016**, *183*, 723–729, doi:10.1007/s00604-015-1718-y.
30. Jahanbani, S.; Benvidi, A. Comparison of two fabricated aptasensors based on modified carbon paste/oleic acid and magnetic bar carbon paste/Fe3O4@oleic acid nanoparticle electrodes for tetracycline detection. *Biosens. Bioelectron.* **2016**, *85*, 553–562, doi:10.1016/j.bios.2016.05.052.
31. Taghdisi, S.M.; Danesh, N.M.; Ramezani, M.; Abnous, K. A novel M-shape electrochemical aptasensor for ultrasensitive detection of tetracyclines. *Biosens. Bioelectron.* **2016**, *85*, 509–514, doi:10.1016/j.bios.2016.05.048.
32. Wong, A.; Scontri, M.; Materon, E.M.; Lanza, M.R.V.; Sotomayor, M.D.P.T. Development and application of an electrochemical sensor modified with multi-walled carbon nanotubes and graphene oxide for the sensitive and selective detection of tetracycline. *J. Electroanal. Chem.* **2015**, *757*, 250–257, doi:10.1016/j.jelechem.2015.10.001.
33. Guo, Y.; Wang, X.; Sun, X. A label-free electrochemical aptasensor based on electrodeposited gold nanoparticles and methylene blue for tetracycline detection. *Int. J. Electrochem. Sci.* **2015**, *10*, 3668–3679.
34. Liu, Y.; Yan, K.; Zhang, J. Graphitic carbon nitride sensitized with CdS quantum dots for visible-light-driven photoelectrochemical aptasensing of tetracycline. *ACS Appl. Mater. Interfaces* **2015**, *2015*, doi:10.1021/acsami.5b08275.
35. Luo, Y.; Xu, J.; Li, Y.; Gao, H.; Guo, J.; Shen, F.; Sun, C. A novel colorimetric aptasensor using cysteamine-stabilized gold nanoparticles as probe for rapid and specific detection of tetracycline in raw milk. *Food Control* **2015**, *54*, 7–15, doi:10.1016/j.foodcont.2015.01.005.
36. Ramezani, M.; Mohammad Danesh, N.; Lavaee, P.; Abnous, K.; Mohammad Taghdisi, S. A novel colorimetric

triple-helix molecular switch aptasensor for ultrasensitive detection of tetracycline. *Biosens. Bioelectron.* **2015**, *70*, 181–187, doi:10.1016/j.bios.2015.03.040.

37. Wang, S.; Liu, J.; Yong, W.; Chen, Q.; Zhang, L.; Dong, Y.; Su, H.; Tan, T. A direct competitive assay-based aptasensor for sensitive determination of tetracycline residue in Honey. *Talanta* **2015**, *131*, 562–569, doi:10.1016/j.talanta.2014.08.028.
38. Liu, B.; Zhang, B.; Chen, G.; Tang, D. Biotin-avidin-conjugated metal sulfide nanoclusters for simultaneous electrochemical immunoassay of tetracycline and chloramphenicol. *Microchim. Acta* **2014**, *181*, 257–262, doi:10.1007/s00604-013-1096-2.
39. Wang, S.; Yong, W.; Liu, J.; Zhang, L.; Chen, Q.; Dong, Y. Development of an indirect competitive assay-based aptasensor for highly sensitive detection of tetracycline residue in honey. *Biosens. Bioelectron.* **2014**, *57*, 192–198, doi:10.1016/j.bios.2014.02.032.
40. Chen, D.; Yao, D.; Xie, C.; Liu, D. Development of an aptasensor for electrochemical detection of tetracycline. *Food Control* **2014**, *42*, 109–115, doi:10.1016/j.foodcont.2014.01.018.
41. Shen, G.; Guo, Y.; Sun, X.; Wang, X. Electrochemical Aptasensor Based on Prussian Blue-Chitosan-Glutaraldehyde for the Sensitive Determination of Tetracycline. *Nano-Micro Lett.* **2014**, *6*, 143–152, doi:10.1007/BF03353778.
42. Que, X.; Chen, X.; Fu, L.; Lai, W.; Zhuang, J.; Chen, G.; Tang, D. Platinum-catalyzed hydrogen evolution reaction for sensitive electrochemical immunoassay of tetracycline residues. *J. Electroanal. Chem.* **2013**, *704*, 111–117, doi:10.1016/j.jelechem.2013.06.023.
43. Conzuelo, F.; Gamella, M.; Campuzano, S.; Reviejo, A.J.; Pingarrón, J.M. Disposable amperometric magneto-immunosensor for direct detection of tetracyclines antibiotics residues in milk. *Anal. Chim. Acta* **2012**, *737*, 29–36, doi:10.1016/j.aca.2012.05.051.
44. Faridah, S.; Azura, N.; Hazana, R.; A.R, G.; Norzaili, Z.; Azima, A.; Zamri, I. Electrochemical sensors for detection of tetracycline antibiotics Unbound free tetracycline and tetracycline conjugates were removed during the washing step Direct competitive ELISA method Carbon working electrode was connected to the electrochemical ayse. *Malaysia Soc. Anim. Prod.* **2012**, *15*, 67–80.
45. Zhang, J.; Wu, Y.; Zhang, B.; Li, M.; Jia, S.; Jiang, S.; Zhou, H.; Zhang, Y.; Zhang, C.; Turner, A.P.F. Label-Free Electrochemical Detection of Tetracycline by an Aptamer Nano-Biosensor. *Anal. Lett.* **2012**, *45*, 986–992, doi:10.1080/00032719.2012.670784.
46. Zhou, L.; Li, D.J.; Gai, L.; Wang, J.P.; Li, Y. Bin Electrochemical aptasensor for the detection of tetracycline with multi-walled carbon nanotubes amplification. *Sensors Actuators, B Chem.* **2012**, *162*, 201–208, doi:10.1016/j.snb.2011.12.067.
47. Wang, H.; Zhao, H.; Quan, X.; Chen, S. Electrochemical Determination of Tetracycline Using Molecularly Imprinted Polymer Modified Carbon Nanotube-Gold Nanoparticles Electrode. *Electroanalysis* **2011**, *23*, 1863–1869, doi:10.1002/elan.201100049.

48. Kim, Y.J.; Kim, Y.S.; Niazi, J.H.; Gu, M.B. Electrochemical aptasensor for tetracycline detection. *Bioprocess Biosyst. Eng.* **2010**, *33*, 31–37, doi:10.1007/s00449-009-0371-4.
49. Jeon, M.; Kim, J.; Paeng, K.J.; Park, S.W.; Paeng, I.R. Biotin-avidin mediated competitive enzyme-linked immunosorbent assay to detect residues of tetracyclines in milk. *Microchem. J.* **2008**, *88*, 26–31, doi:10.1016/j.microc.2007.09.001.
50. Zhang, Y.; Lu, S.; Liu, W.; Zhao, C.; Xi, R. Preparation of anti-tetracycline antibodies and development of an indirect heterologous competitive enzyme-linked immunosorbent assay to detect residues of tetracycline in milk. *J. Agric. Food Chem.* **2007**, *55*, 211–218, doi:10.1021/jf062627s.
51. Mohammad-Razdari, A.; Ghasemi-Varnamkhasti, M.; Rostami, S.; Izadi, Z.; Ensafi, A.A.; Siadat, M. Development of an electrochemical biosensor for impedimetric detection of tetracycline in milk. *J. Food Sci. Technol.* **2020**, *57*, 4697–4706, doi:10.1007/s13197-020-04506-2.
52. Lorenzetti, A.S.; Sierra, T.; Domini, C.E.; Lista, A.G.; Crevillen, A.G.; Escarpa, A. Electrochemically Reduced Graphene Oxide-Based Screen-Printed Electrodes for Total Tetracycline Determination by Adsorptive Transfer Stripping. *Sensors* **2020**, *20*, 1–12.
53. Abraham, T.; Gigimol, M.G.; Priyanka, R.N.; Susan, M.; Korah, B.K.; Mathew, B. In-situ fabrication of Ag3PO4 based binary composite for the efficient electrochemical sensing of tetracycline. *Mater. Lett.* **2020**, *279*, 128502, doi:10.1016/j.matlet.2020.128502.
54. Allahverdiyeva, S.; Yardım, Y.; Senturk, Z. Electrooxidation of tetracycline antibiotic demeclocycline at unmodified boron-doped diamond electrode and its enhancement determination in surfactant-containing media. *Talanta* **2021**, *223*, 121695, doi:10.1016/j.talanta.2020.121695.
55. Turbale, M.; Moges, A.; Dawit, M.; Amare, M. Adsorptive stripping voltammetric determination of Tetracycline in pharmaceutical capsule formulation using Poly (Malachite green) modified glassy carbon electrode. *Heliyon* **2020**, *6*, e05782, doi:10.1016/j.heliyon.2020.e05782.
56. El Alami El Hassani, N.; Baraket, A.; Boudjaoui, S.; Taveira Tenório Neto, E.; Bausells, J.; El Bari, N.; Bouchikhi, B.; Elaissari, A.; Errachid, A.; Zine, N. Development and application of a novel electrochemical immunosensor for tetracycline screening in honey using a fully integrated electrochemical Bio-MEMS. *Biosens. Bioelectron.* **2019**, *130*, 330–337, doi:10.1016/j.bios.2018.09.052.
57. Calixto, C.M.F.; Cavalheiro, É.T.G. Determination of Tetracycline in Bovine and Breast Milk Using a Graphite–Polyurethane Composite Electrode. *Anal. Lett.* **2017**, *50*, 2323–2334, doi:10.1080/00032719.2017.1283506.
58. Kesavan, S.; Kumar, D.R.; Lee, Y.R.; Shim, J.J. Determination of tetracycline in the presence of major interference in human urine samples using polymelamine/electrochemically reduced graphene oxide modified electrode. *Sensors Actuators, B Chem.* **2017**, *241*, 455–465, doi:10.1016/j.snb.2016.10.091.
59. Kushikawa, R.T.; Silva, M.R.; Angelo, A.C.D.; Teixeira, M.F.S. Construction of an electrochemical sensing platform based on platinum nanoparticles supported on carbon for tetracycline determination. *Sensors*

Actuators, B Chem. **2016**, *228*, 207–213, doi:10.1016/j.snb.2016.01.009.

60. Calixto, C.M.F.; Cavalheiro, É.T.G. Determination of Tetracyclines in Bovine and Human Urine using a Graphite-Polyurethane Composite Electrode. *Anal. Lett.* **2015**, *48*, 1454–1464, doi:10.1080/00032719.2014.984194.
61. Gan, T.; Shi, Z.; Sun, J.; Liu, Y. Simple and novel electrochemical sensor for the determination of tetracycline based on iron/zinc cations-exchanged montmorillonite catalyst. *Talanta* **2014**, *121*, 187–193, doi:10.1016/j.talanta.2014.01.002.
62. Asadollahi-Baboli, M.; Mani-Varnosfaderani, A. Rapid and simultaneous determination of tetracycline and cefixime antibiotics by mean of gold nanoparticles-screen printed gold electrode and chemometrics tools. *Meas. J. Int. Meas. Confed.* **2014**, *47*, 145–149, doi:10.1016/j.measurement.2013.08.029.
63. Conzuelo, F.; Campuzano, S.; Gamella, M.; Pinacho, D.G.; Reviejo, A.J.; Marco, M.P.; Pingarrón, J.M. Integrated disposable electrochemical immunosensors for the simultaneous determination of sulfonamide and tetracycline antibiotics residues in milk. *Biosens. Bioelectron.* **2013**, *50*, 100–105, doi:10.1016/j.bios.2013.06.019.
64. Calixto, C.M.F.; Cervini, P.; Cavalheiro, É.T.G. Determination of tetracycline in environmental water samples at a graphite-polyurethane composite electrode. *J. Braz. Chem. Soc.* **2012**, *23*, 938–943, doi:10.1590/S0103-50532012000500020.
65. Wang, H.; Zhao, H.; Quan, X. Gold modified microelectrode for direct tetracycline detection. *Front. Environ. Sci. Eng. China* **2012**, *6*, 313–319, doi:10.1007/s11783-011-0323-5.
66. Casella, I.G.; Fabio, P. Determination of tetracycline residues by liquid chromatography coupled with electrochemical detection and solid phase extraction. *J. Agric. Food Chem.* **2009**, *57*, 8735–8741, doi:10.1021/jf902086y.
67. Guo, G.; Zhao, F.; Xiao, F.; Zeng, B. Voltammetric determination of tetracycline by using multi-wall carbon nanotube - ionic liquid film coated glassy carbon electrode. *Int. J. Electrochem. Sci.* **2009**, *4*, 1365–1372.
68. Masawat, P.; Slater, J.M. The determination of tetracycline residues in food using a disposable screen-printed gold electrode (SPGE). *Sensors Actuators, B Chem.* **2007**, *124*, 127–132, doi:10.1016/j.snb.2006.12.010.
69. Vega, D.; Agüí, L.; González-Cortés, A.; Yáñez-Sedeño, P.; Pingarrón, J.M. Voltammetry and amperometric detection of tetracyclines at multi-wall carbon nanotube modified electrodes. *Anal. Bioanal. Chem.* **2007**, *389*, 951–958, doi:10.1007/s00216-007-1505-7.
70. Cai, Y. e.; Cai, Y.; Shi, Y.; Mou, S.; Lu, Y. Optimizing the integrated pulsed amperometric multicycle step waveform for the determination of tetracyclines. *J. Chromatogr. A* **2006**, *1118*, 35–40, doi:10.1016/j.chroma.2005.11.091.
71. Treetepvijit, S.; Preechaworapun, A.; Praphairaksit, N.; Chuanuwatanakul, S.; Einaga, Y.; Chailapakul, O. Use of nickel implanted boron-doped diamond thin film electrode coupled to HPLC system for the determination of tetracyclines. *Talanta* **2006**, *68*, 1329–1335, doi:10.1016/j.talanta.2005.07.047.

72. Charoenraks, T.; Chuanuwatanakul, S.; Honda, K.; Yamaguchi, Y.; Chailapakul, O. Analysis of tetracycline antibiotics using HPLC with pulsed amperometric detection. *Anal. Sci.* **2005**, *21*, 241–245, doi:10.2116/analsci.21.241.
73. Pellegrini, G.E.; Carpico, G.; Coni, E. Electrochemical sensor for the detection and presumptive identification of quinolone and tetracycline residues in milk. *Anal. Chim. Acta* **2004**, *520*, 13–18, doi:10.1016/j.aca.2004.04.052.
74. Zhao, F.; Zhang, X.; Gan, Y. Determination of tetracyclines in ovine milk by high-performance liquid chromatography with a coulometric electrode array system. *J. Chromatogr. A* **2004**, *1055*, 109–114, doi:10.1016/j.chroma.2004.08.131.
75. Loetanantawong, B.; Suracheep, C.; Somasundrum, M.; Surareungchai, W. Electrocatalytic Tetracycline Oxidation at a Mixed-Valent Ruthenium Oxide-Ruthenium Cyanide-Modified Glassy Carbon Electrode and Determination of Tetracyclines by Liquid Chromatography with Electrochemical Detection. *Anal. Chem.* **2004**, *76*, 2266–2272, doi:10.1021/ac035085b.
76. Wangfuengkanagul, N.; Siangproh, W.; Chailapakul, O. A flow injection method for the analysis of tetracycline antibiotics in pharmaceutical formulations using electrochemical detection at anodized boron-doped diamond thin film electrode. *Talanta* **2004**, *64*, 1183–1188, doi:10.1016/j.talanta.2004.04.032.
77. Dang, X.; Hu, C.; Wei, Y.; Chen, W.; Hu, S. Sensitivity improvement of the oxidation of tetracycline at acetylene black electrode in the presence of sodium dodecyl sulfate. *Electroanalysis* **2004**, *16*, 1949–1955, doi:10.1002/elan.200403049.
78. Charoenraks, T.; Palaharn, S.; Grudpan, K.; Siangproh, W.; Chailapakul, O. Flow injection analysis of doxycycline or chlortetracycline in pharmaceutical formulations with pulsed amperometric detection. *Talanta* **2004**, *64*, 1247–1252, doi:10.1016/j.talanta.2004.04.036.
79. Agüí, L.; Guzman, A.; Pedrero, M.; Yáñez-Sedeño, P.; Pingarrón, J.M. Voltametric and flow injection determination of oxytetracycline residues in food samples using carbon fiber microelectrodes. *Electroanalysis* **2003**, *15*, 601–607, doi:10.1002/elan.200390075.
80. Palaharn, S.; Charoenraks, T.; Wangfuengkanagul, N.; Grudpan, K.; Chailapakul, O. Flow injection analysis of tetracycline in pharmaceutical formulation with pulsed amperometric detection. *Anal. Chim. Acta* **2003**, *499*, 191–197, doi:10.1016/S0003-2670(03)00948-6.
81. Zhou, J.; Gerhardt, G.C.; Baranski, A.; Cassidy, R. Capillary electrophoresis of some tetracycline antibiotics coupled with reductive fast cyclic voltammetric detection. *J. Chromatogr. A* **1999**, *839*, 193–201, doi:10.1016/S0021-9673(99)00152-1.
82. Kazemifard, A.G.; Moore, D.E. Evaluation of amperometric detection for the liquid-chromatographic determination of tetracycline antibiotics and their common contaminants in pharmaceutical formulations. *J. Pharm. Biomed. Anal.* **1997**, *16*, 689–696, doi:10.1016/S0731-7085(97)00089-7.
83. Oungpipat, W.; Southwell-Keely, P.; Alexander, P.W. Flow injection detection of tetracyclines by electrocatalytic oxidation at a nickel-modified glassy carbon electrode. *Analyst* **1995**, *120*, 1559–1565,

doi:10.1039/an9952001559.

84. Hou, W.; Wang, E. Liquid chromatographic determination of tetracycline antibiotics at an electrochemically pre-treated glassy carbon electrode. *Analyst* **1989**, *114*, 699–702, doi:10.1039/AN9891400699.
85. Pinilla Gil, E.; Calvo Blazquez, L.; Garcia-Monco Carra, R.M.; Sanchez Misiego, A. Determination of oxytetracycline in urine and human serum by differential pulse polarography. *Fresenius Zeitschrift für Anal. Chemie* **1989**, *335*, 1002–1004.
86. Ji, H.; Wang, E. Flow injection amperometric detection based on ion transfer across a water - Solidified nitrobenzene interface for the determination of tetracycline and terramycin. *Analyst* **1988**, *113*, 1541–1543, doi:10.1039/AN9881301541.
87. Sabharwal, S.; Kishore, K.; Moorthy, P.N. Determination of tetracycline hydrochloride in presence of anhydrotetracycline by differential pulse polarography. *J. Pharm. Sci.* **1988**, *77*, 78–80, doi:10.1002/jps.2600770115.
88. Pinilla Gil, E.; Calvo Blázquez, L.; García-Moncó Carra, R.M.; Sánchez Misiego, A. Adsorptive stripping voltammetry of oxytetracycline at the hanging mercury drop electrode (HMDE) in acid medium. *Fresenius Zeitschrift für Anal. Chemie* **1988**, *332*, 821–822, doi:10.1007/BF01129787.
89. Wang, E.; Liu, Y. Cyclic voltammetry and chronopotentiometry with cyclic linear current scanning of terramycin at the water/nitrobenzene interface. *J. Electroanal. Chem.* **1986**, *214*, 459–464, doi:10.1016/0022-0728(86)80114-0.
90. Chatten, L.G.; Fleischmann, M.; Pletcher, D. THE ANODIC OXIDATION OF SOME TETRACYCLINES. *J. Electroanal. Chem.* **1979**, *102*, 407–413.